Structural studies of several distinct meta-stable forms of amorphous ice

C. A. Tulk,[*,1] C. J. Benmore,[†,1] J. Urquidi, [†] D. D. Klug,[‡] J. Neuefeind, [†]
B. Tomberli[§] and P. A. Egelstaff[§]

[*] Oak Ridge National Laboratory, Oak Ridge TN, 37831
[†]Argonne National Laboratory, Argonne IL, 60439
[‡]National Research Council of Canada, Ottawa Ontario K0A 0R6
[§] Dept. of Physics, University of Guelph, Guelph Ontario Canada, N1G 2W1

Abstract: Structural changes during annealing of *high-density amorphous* ice are studied using both neutron and x-ray diffraction. The first diffraction peak was followed from the high-density to the low-density amorphous form. Changes were observed to occur through a series of *intermediate* forms that appear to be *meta-stable at each anneal temperature*. Five distinct amorphous forms have been studied using neutron scattering, and an infinite number may be possible. Radial distribution functions indicate that the structure evolves systematically between 4 and 8 Å. The phase transformations in low temperature liquid water may be much more complex than currently understood.

[1] These authors contributed equally to this work.

Pressurization of ice I to approximately 13 kbar is known to yield the most common high density amorphous (HDA) form of ice, [1] while low pressure vapor deposition onto a cold target, [2] rapid quenching of the liquid, [3] or decompression/heating the HDA form are known to produce other amorphous forms, all with densities that are similar to the crystalline ice I phase, they have been categorized as low density amorphous (LDA) forms. In addition, the LDA form has been reported to abruptly and reversibly transform into the HDA form with the application of pressure, possibly through a first order phase transition.[4] This has lead to the suggestion that all forms of amorphous water can be partitioned into these two high-density and low-density forms.[5] However, a survey of the literature provides the seemingly contradictory view that a continuous range of amorphous structures may exist.[6,7,8,9,10] In fact, Mishima et. al[1] in their original work on the crystalline to amorphous transition stated that, "Heating below the 117 K transition causes irreversible changes in the diffraction pattern…", thus suggesting the possibility of many amorphous forms. HDA ice may therefore exist in a separate "megabasin" [11] in the potential energy surfaces of the amorphous ices. However, no detailed structural studies of these possible intermediate forms have ever been reported, thus the interpretation of the nature of this very important transition is very difficult.

Calorimetric studies of this transition have indicated a sharp exothermic peak associated with the HDA to LDA transition at 113.4 K at a heating rate of 10 K h^{-1}. There was evidence, however, that suggested slow exothermal processes may be occurring at lower temperature and this was attributed to possible annealing of the sample, but no structural studies of this process have ever been reported.[12] In addition, Raman and infrared spectroscopic studies have indirectly indicated the possibility of very subtle differences in the local hydrogen bonding structure among several low-density phases produced by the various methods.[1314] These differences have, however, been accepted as only minor variations of the more general LDA structural category, and similar claims have been made regarding the HDA category.[7] Structural studies of these various amorphous polymorphs, particularly by neutron/x-ray diffraction[15,16,17,18] have highlighted the many differences between the high-density and low-density amorphous forms, and have also

led to the suggestion that liquid water can be considered a mixture of low-density and high-density forms.[19] Conversely however, relaxation, as indicated by the shift in the first diffraction peak in the high-density amorphous form of D_2O upon annealing, has also led to the suggestion that some variation in the HDA structure may exist. However, such states were thought to be transient in nature at the formation temperature during the HDA to LDA transformation.[7] Detailed structural evidence for the existence of meta-stable intermediate forms has not been reported so far.

Here we have studied the structural changes during the transition in detail using both neutron and x-ray scattering. We have followed the transition continuously by recording the position of the first sharp diffraction peak in the neutron and x-ray static structure factor as a function of time at several anneal temperatures. It is shown that the transition from the high-density form to the low-density form can occur continuously through a series of amorphous forms that appear to be intermediate and *meta-stable at each anneal temperature* over the course of several hours (with every indication that these forms are metastable for much longer times). At each anneal temperature below 110 K the transition proceeds rapidly at first (possibly through transient structures), but then becomes kinetically inhibited with no further structural evolution. In all, using neutron diffraction we have studied five metastable amorphous ice forms. More importantly however, we have subsequently compared data from each structure at 40K and, using the derived neutron and x-ray radial distribution functions, have identified the major structural changes that occur between each successive metastable form during the HDA $\rightarrow$ LDA transformation.

High-density amorphous ice (99.999% D_2O for neutron studies and 99.99 % H_2O for x-ray studies) was formed by pressurizing ice Ih to 18 kbar at 77K in a piston cylinder apparatus at the National Research Council of Canada. These samples were stored in liquid nitrogen during shipment to Argonne National Laboratory. The neutron diffraction data was collected using the Glass Liquids and Amorphous materials Diffractometer at the Intense Pulsed Neutron Source. Subsections of the samples were placed in a vanadium container and loaded into a pre-cooled *(orange)* cryostat. The loading

procedure was carried out at 77 K. The data was analyzed using the ATLAS software package that corrected for background scattering from the empty vanadium can, absorption, multiple scattering and was normalized to an absolute scale using the isotropic incoherent scattering from vanadium. The resulting differential cross section was then normalized to the high momentum transfer limit (i.e. up to a Q_{max} of 25 $Å^{-1}$). This corrected for the unknown effective density of the powdered sample. Finally the inelastically scattered (Placzek) component was calculated and removed, giving the total neutron static structure factor $S_N(Q)$. Samples used for the x-ray experiments were transferred from liquid nitrogen storage into a cryostat mounted on the high-energy x-ray diffractometer at the 11-ID-C beamline at the Advanced Photon Source.[20] The sample was loaded into an aluminum holder with thin kapton windows. The x-ray measurements were made in transmission geometry with the incident beam energy of 98 keV and scattering from four millimeter thick samples. The procedure for correcting the data has been outlined in detail in previous work.[21] The x-ray data presented have been corrected for detector dead time, container scattering, varying detector distance and polarization, and have been normalized to the sum of the elastic plus Compton scattering with a Klein-Nishina correction. Multiple scattering and attenuation corrections for this sample were found to be negligible (~1%) at this energy. For both the x-ray and neutron data the sample temperature was accurate to within ~ 0.1 K through the use of a low-density helium exchange gas. The total radial distribution function G(r) is related to the Fiber-Ziman structure factor by the Fourier transform, $S(Q) = 1 + \frac{4\pi\rho}{Q}\int r[G(r)-1]\sin(Qr)dr$, where ρ is the density of the sample in atoms per cubic angstrom. The densities for the HDA and LDA were taken from the literature[1] and the densities of the quenched intermediate phases were determined by the scaled ratio of the position of the first diffuse peak position to the total peak shift between the HDA and LDA data.

After loading the samples at low temperature into the neutron and x-ray diffractometers, they were initially cooled to 40 K and a data set collected from the unannealed samples. The fully corrected total x-ray and neutron structure factor functions from the unannealed samples are given in the lower traces of Figure 1 (a) and (b). The high quality of the

samples is demonstrated by the absence of intense crystalline ice Bragg peaks. For the unannealed phases the first peak position in the neutron structure factor is measured at a momentum transfer of 2.11 $Å^{-1}$; while, the first peak position in the x-ray structure factor is measured at a momentum transfer of 2.25 $Å^{-1}$. Previously, these peaks had been measured at 2.15 $Å^{-1}$ in both the neutron and x-ray structure factors.[15, 16, 17]

The samples were then annealed at 95, 100, 105 and 110 K for the times specified in Figures 2 and 3. Structural changes during each isothermal annealing period were partially characterized by recording the position of the FSDP in the structure factor. After some time no further structural evolution was apparent, i.e. when the slope of the curves through the FSDP position as a function of time is zero, Figure 2 and 3, therefore suggesting that a meta-stable structure had been formed at each anneal temperature. The temperature was then reduced to 40 K for comparison of S(Q)'s among amorphous forms. The temperature was then increased for the next isothermal annealing cycle. Several of the neutron and x-ray S(Q) functions collected at 40 K are shown in Figure 1.

The FSDP peak positions in the neutron S(Q) are given as a function of total anneal time for each isothermal anneal temperature in Figure 2, and likewise those from the x-ray S(Q) are given in Figure 3. The temperature dependence of the neutron FSDP has been measured and shown to change from 1.95±0.02 $Å^{-1}$ to 1.93 ±0.02 $Å^{-1}$ upon cooling from 105 K to 40K. Therefore temperature and thermal expansion can be excluded as a possible cause of the peak shift in these plots. It is clear from these data that there are no sharp discontinuities in the peak position during the transformation, and thus we conclude that, (at the local structure level) amorphous ice can clearly evolve continuously from the high-density form to the low-density form. During the 110 K anneal the sample overcomes the remaining potential barriers and the structure evolves toward that with an energy very near the minimum in the *amorphous ice "megabasin"* [11] in the potential energy surfaces of the amorphous ices, and thus results in the lowest density, or LDA, structure. We note that the structure after an isothermal anneal, at any given anneal temperature, may not be identical from sample to sample. This is due to the fact that the transition is highly exothermic, and therefore the degree of structural evolution may

depend on the packing morphology and the efficiency of the heat transport mechanism (i.e. low pressure He exchange gas in this case), these conditions are very difficult to reproduce from experiment to experiment. Furthermore, if the heat removal mechanism is not sufficiently efficient the transition may continue to the LDA form and thus appear to occur though a series of transient rather than meta-stable amorphous forms.

In addition to the unannealed HDA and final LDA form, three other distinct intermediate forms have been studied at 40K using neutron diffraction. The trend in Figure 1(a) is clear, in the neutron S(Q) the FSDP progresses toward lower momentum transfer with increasing anneal temperature, from 2.11 to 2.06 to 1.92 and finally to 1.67 $Å^{-1}$ in the low density amorphous phase. This is accompanied by an increasing peak intensity (atom-atom correlations) at ~ 2.85 $Å^{-1}$ and a shift to lower momentum transfer of the broad peak seen from 4.0 $Å^{-1}$ to 3.63 $Å^{-1}$. The x-ray structure factor, in Figure 1(b), shows a similar trend, the FSDP position also shifts toward lower momentum transfer, from 2.25 to 2.16 to 2.09 and finally to 1.71 $Å^{-1}$, for the phases shown. Also shown is an initial decrease in the x-ray FSDP intensity, followed by an increase in intensity and significant sharpening in the final LDA phase. This is accompanied by a significant increase in the intensity of the peaks at 3.05 $Å^{-1}$ and 4.75 $Å^{-1}$. The general features of both the unannealed HDA and the final LDA structure factors from x-ray and neutron scattering agree very well with those recorded previously,[15,16,17] with however, the exception of the intensity of the second peak in the reported x-ray HDA S(Q) measurement,[16] which is closer to that measured in the LDA form. This may indicate that the previously measured x-ray S(Q) could have resulted from a partially annealed HDA structure. Careful evaluation of the data showed that the S(Q) functions from each intermediate form are distinct, i.e. they cannot be reproduced by any linear combination of the HDA and LDA S(Q) functions.

The measured total structure factors of the quenched states have been transformed into real-space radial distribution functions and the several representative data sets plotted in Figure 4 (a) for the neutron experiments, and Figure 4 (b) for the x-ray experiments. While the neutron data are predominantly weighted toward the hydrogen – hydrogen and oxygen – hydrogen correlations and the x-ray data are predominantly weighted toward

the oxygen – oxygen correlations, the major real-space structural trends upon annealing can be seen in both sets of data, and are generally described by short to intermediate range structural changes between 4 and 8 Å. The broad peak centered on ~ 6.4 Å shifts systematically to greater distance with increasing anneal temperature. In addition, a significant increase in the intensity of the broad peak centered at ~ 4.5 Å with increasing anneal temperature is noted. The hydrogen bonded oxygen – oxygen distance, given by the position of the first peak in the x-ray G(r), shortens systematically through the transformation between each amorphous form and ranges from 2.80 Å in the unannealed HDA phase to 2.76 Å in the final lowest density phase, we note that this is consistent with measured Raman data.[22]

In conclusion, we have annealed HDA ice at several temperatures below 113.4 K, i.e. the recorded transition temperature to the LDA form. It is clear from the position of the FSDP in the static structure factor that the transition from the high-density amorphous form to the low-density amorphous form can proceed in a structurally continuous manner through a series of intermediate, apparently meta-stable amorphous forms. Several of these meta-stable forms have been observed and detailed radial distribution functions compared at T = 40 K. It is quite reasonable to expect that, in principle, a continuous distribution of recoverable forms between HDA and LDA ice are possible. At any T < 113.4 K, the thermal energy is insufficient to overcome the potential barriers that define a particular metastable structure. This is exactly what is in general expected for the existence of any metastable phase. This indicates that the transformation between the *poly-amorphs* of ice may be somewhat complex. From the radial distributions functions presented here, it appears that the transition predominantly evolves on the short to intermediate length scale, i.e. with major structural changes occurring between 4 and 8 Å and more subtle changes also occur on the hydrogen bond length scale. These data may have significant implications regarding the current understanding of the structural relationship between a low-density liquid water (LDL water) and LDA ice, and a high-density liquid water (HDL water) and high-density amorphous HDA ice.[2,23,24,25] In addition, understanding structural variations in amorphous water, particularly the

predominant length scales over which such variations occur, may provide a basis for understanding bio-molecular hydration and cryo-preservation.

[1] O. Mishima, L.D. Calvert, E. Whalley, Nature, **310**, 393 (1984).

[2] E. F. Burton, W.F. Oliver, Proc. R. Soc. Lond. A **153**, 166 (1936).

[3] E. Mayer, J. Appl. Phys **58**, 663 (1985).

[4] O. Mishima, J. Chem. Phys. **100**, 5910 (1994).

[5] O. Mishima, H.E. Stanley, Nature **396**, 329 (1998).

[6] E. Whalley, O. Mishima, Y.P. Handa, D.D. Klug, Annals N.Y. Acad. Sci., 484, 81 (1986).

[7] H. Schober, et al., Physica B, **241-243,** 897 (1998).

[8] G.P. Johari, A. Hallbrucker, E. Mayer, Science **273**, 90 (1996).

[9] T. Loerting, C. Salzmann, I. Kohl, E. Mayer, A. Hallbruker, Physical Chemistry: Chemical Physics, **3**, 5355 (2001).

[10] O. Mishima, Nature, **384**, 546 (1996).

[11] C.A., Angell, Science **267**, 1924 (1995).

[12] Y.P. Handa, O. Mishima, E. Whalley, J. Chem. Phys. **84**, 2766 (1986).

[13] C.A. Tulk, D.D. Klug, R. Branderhorst, P. Sharpe, J.A. Ripmeester, J. Chem. Phys. **109**, 8478 (1998).

[14] E. Mayer, J. Phys. Chem., **89**, 3474 (1985).

[15] M.A. Floriano, E. Whalley, E. Svensson, V.F. Sears, Phys. Rev. Lett., **57**, 3062 (1986).

[16] A. Bizid, L. Bosio, A. Defrain, M. Oumezzine, J. Chem. Phys., **87**, 2225 (1987).

[17] M.C. Bellissent-Funel, J. Teixeira, L. Bosio, J. Chem. Phys., **87**, 2231 (1987).

[18] M.C. Bellissent-Funel, L. Bosio, A. Hallbruker, E. Mayer, R. Sridi-Dorbez, J. Chem. Phys., **97**, 1282 (1992).

[19] O. Mishima, Nature, **396**, 329 (1998).

[20] U. Rütt, et al. Nucl. Instr. Meth. A, in press.

[21] B. Tomberli, C. J. Benmore, P.A. Egelstaff, J. Neuefeind, V. Honlimaki, J. Phys.: Condens. Matter, **12**, 2597 (2000).

[22] D.D. Klug, O. Mishima, E. Whalley, J. Chem. Phys., **86**, 5323 (1987).

[23] M.-C. Bellissent-Funel, Europhys Lett., **42**, 161 (1998).

[24] F.W. Starr, M.-C. Bellissent-Funel, H.E. Stanley, Phys. Rev. E., **60**, 1084 (1999).

[25] A.K. Soper, M.A. Ricci, Phys. Rev. Lett., **84**, 2881(2000).

Figure 1

Total neutron S(Q) from D_2O (a) and x-ray S(Q) from H_2O (b) of several amorphous ice forms. Data were recorded at T=40K after each anneal. Neutron data sets were collected for 12 hours and X-ray data sets were collected for 3 hours. Solid lines in (a) are the smoothed functions. This data were used to obtain the radial distribution functions plotted in Figure 4 (where Q_{max} = 25 $Å^{-1}$).

Figure 2

The position of the first sharp diffraction peak (FSDP) in the neutron structure factor as a function of total anneal time. After each isothermal anneal the samples were cooled to 40 K for structural comparison, see Figure 1. The unannealed state corresponds with the high-density amorphous phase. The solid curves were drawn to aid the eye. It is likely that pressurization of ice I at lower temperatures will result in a slightly different structure.

Figure 3

The position of the first sharp diffraction peak (FSDP) in the x-ray structure factor as a function of total anneal time. The results from two samples are plotted. Data from the second sample are indicated after 3000 minutes during transformation to the low-density form after warming above 110K. The solid horizontal lines represent the measured position of the first diffraction peak in the high-density form and the low-density form. As with the neutron data, the structures were cooled to 40 K after each anneal structural comparison. The solid curves are drawn to aid the eye.

Figure 4

The neutron radial distribution functions (a) and the x-ray radial distribution functions (b) calculated from data presented in Fig 1. The densities used in the transforms were 0.1174, 0.1146, 0.1078 and 0.09434 atoms/$Å^3$ for the progression from HDA to LDA in the neutron scattering case, and 0.1174, 0.1110, 0.1107, 0.09434 atoms/$Å^3$ for the x-ray scattering experiments.

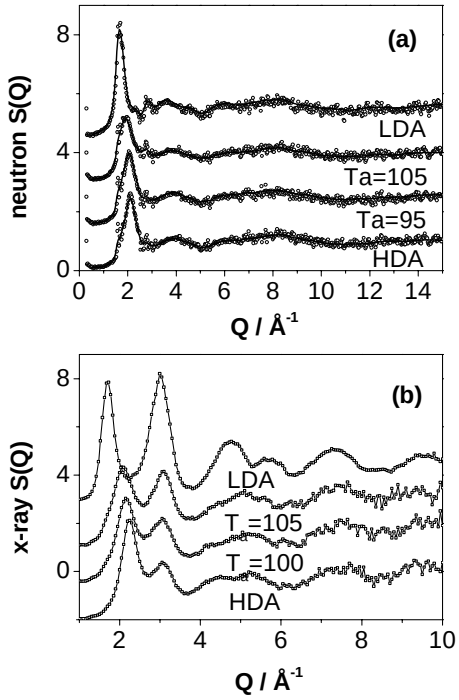
(a)
neutron S(Q)
LDA
Ta=105
Ta=95
HDA
Q / Å-1
(b)
x-ray S(Q)
LDA
T =105
T =100
HDA
Q / Å-1

Figure 1

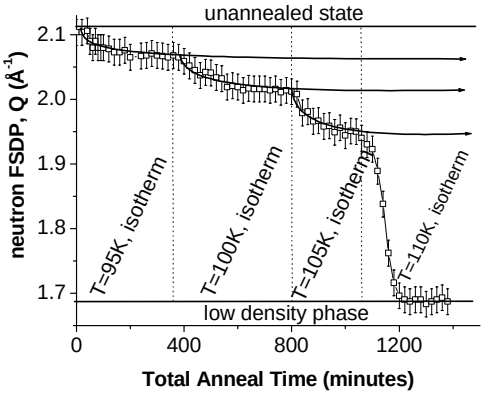
unannealed state
2.1
2.0
1.9
1.8
1.7
neutron FSDP, Q (Å^{-1})
T=95K, isotherm
T=100K, isotherm
T=105K, isotherm
T=110K, isotherm
low density phase
0
400
800
1200
Total Anneal Time (minutes)

Figure 2

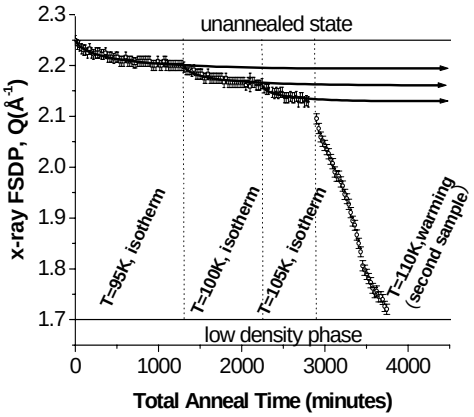
unannealed state
low density phase
T=95K, isotherm
T=100K, isotherm
T=105K, isotherm
T=110K,warming
(second sample)
x-ray FSDP, Q(Å-1)
Total Anneal Time (minutes)
2.3
2.2
2.1
2.0
1.9
1.8
1.7
0
1000
2000
3000
4000

Figure 3

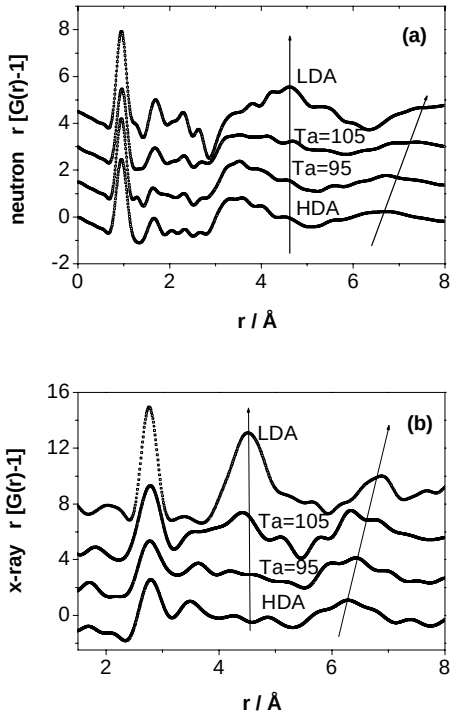
(a)
LDA
Ta=105
Ta=95
HDA
neutron r [G(r)-1]
r / Å
(b)
LDA
Ta=105
Ta=95
HDA
x-ray r [G(r)-1]
r / Å

Figure 4